CHAPTER V
0-3 CONNECTIVITY OF PVDF/BST PIEZOELECTRIC COMPOSITES

5.1 Abstract

Film mechanical sensors, one of the piezoelectric applications, which are focused on this research, are used to measure or detect various mechanical quantities. This work extended the range of material properties by fabricating PVDF/ $Ba_{0.7}Sr_{0.3}TiO_3$ composite film. The $Ba_{0.7}Sr_{0.3}TiO_3$ as piezoelectric ceramic is induced in composite to increase the dielectric constant and piezoelectric properties. A certain weight fraction of 0.3, 0.5 and 0.7 of barium strontium titanate ($Ba_{0.7}Sr_{0.3}TiO_3$) powder at different calcining temperatures was embedded in a matrix of poly vinylidene fluoride (PVDF) before compression molding into 100-200 μm thick sheets. The crystal phase of PVDF, $Ba_{0.7}Sr_{0.3}TiO_3$ and composite is investigated. Subsequently, thermal properties at differential %wt of the ceramic were studied. The microstructure of the composite was observed using scanning electron microscopy (SEM). The dielectric constant and the loss tangent of composites at different %wt and calcined temperature of ceramic were also investigated.

5.2 Introduction

Polymer/ceramic composites have received much attention as new piezoelectric materials for applications in electromechanical transducer, such as microphones, hydrophones, medical ultrasound and pyroelectric detector, *etc*[Olszowy, M. (1997)]. Poly vinylidene fluoride (PVDF) was used as a piezoelectric polymer matrix. The dielectric constant of PVDF is higher than most polymers, and makes PVDF attractive for integration into devices as the signal to noise ratio is less for higher dielectric materials. The weak points of PVDF are possessed low the dielectric constant compare to those of ceramic and exhibit relaxation behavior. From these concerns, the composite of PVDF and ceramic with high dielectric constant would be expected to have higher dielectric constant and less relaxation behavior.

Barium strontium titanate (BST) was used as ferroelectric ceramic. BST is the solid solution of $BaTiO_3$ and $SrTiO_3$, which belong to the general class of ferroelectric materials based on the perovskite structure [Wua, D., *et al.* 2000]. Barium titanate ($BaTiO_3$) and its related compounds have been extensively used in the preparation of high dielectric capacitors, positive temperature coefficient (PTC) resistors, transducers and ferroelectric memories. The substitution of strontium for barium and desirable properties can be obtained such as high dielectric permitivity and low loss factor at room temperature. The weak points of BST are hard fabrication and low dielectric break down. By mixing BST in a polymer matrix, the dielectric breakdown and the difficulty in fabrication would be improved. Variety of barium titanate (BT) composites has already been done by many research groups. However BST which offers superior properties than those of BT still shows less work in composite field. The simplest fabrication of PVDF/BST composites is the composites of 0-3 connectivity. To design a polymer/ceramic composite, a fine powder is dispersed in a PVDF matrix [Lu, Q. *et al.,* (2004)]. The composites are mainly characterized for the microstructure, thermal properties, and dielectric properties. These composite would be promising for electronic application due to the characteristics of lead-free, low-cost, light weight, and high dielectric constant.

5.3 Experimental

Barium Strontium Titante Preparation

$Ba_{0.7}Sr_{0.3}TiO_3$ powder was prepared by sol-gel process. Equal moles of barium acetate and strontium acetate were dissolved separately into methyl alcohol 20 ml in the presence of glacial acetic acid 10 ml. The solutions were then mixed and stirred for 20 minutes at room temperature. The prescribed amount of titanium-n-butoxide was added into the mixture. All the materials mentioned above were thoroughly mixed to prepare a stable solution with uniform composition until gel solution occurs. After that the gel solution was poured into an alumina crucible and heated by using a 2-step thermal decomposition method with different calcining

temperatures 800 and 1000 in order to decompose the precursors and to crystallize the barium strontium titanate and investigate the dielectric properties of composites.

PVDF/Barium Strontium Titante composite Preparation

PVDF powder supplied by Solvay (Solef 1008) was dissolved in dimethly formamide (DMF) at 60°C. For composite preparation the polymer/solvent ratio was 10g/100 ml. Proportionate quantity of $Ba_{0.7}Sr_{0.3}TiO_3$ powder at different calcining temperature was added in the polymer solution. It was homogenized by magnetic stirrer. Additional mixing by ultrasonic was used to guarantee that the powder agglomerated were broken. The solution was dried by heating at 100 °C. The composite film was prepared by a Wabash compression as pressing dried solution at 174 ° C for 20 minutes under pressure of 10 tons. The thickness of the prepared films was ranged between 100-200 μm. Following the above method, the composite films of 30, 50 and 70% by weight ceramic were fabricated.

Characterization

The crystal phase of PVDF and perovskite structure of the $Ba_{0.7}Sr_{0.3}TiO_3$ powders at different calcining temperatures were obtained using X-ray diffraction (XRD, Rigaku, model Dmax 2002). Thermo gravimetric analysis (TGA) was performed using a TG-DTA pyres Diamond (Perkin Elmer). The mass change with increasing temperature was monitored and recorded from 30°C to 1200°C with a heating rate of 20°C/min under N_2 flow. The distribution of ceramic powders in composites and morphology of ceramic were observed using scanning electron microscope (SEM; JSM-5200, JEOL). The particle size of calcined powder was observed using transmission electron microscope (TEM 100 keV, JEOL, model MJEM-1230). Finally, the dielectric properties of the specimens of composites and ceramic were measured using Hewlett-Packard 4194A impedance/gain phase analyzer. The measurements were performed at room temperature with a frequency range of 1 kHz-10 MHz.

5.4 Results and Discussions

5.4.1 X-ray diffraction (XRD)

Figure 5.1 shows the x-ray diffraction patterns of undrawn PVDF film. From XRD pattern of PVDF, the peaks in 2θ Bragg angle with values of 20, 27 and 40 corresponding to the plane [(1 1 0),(0 2 1),(0 0 2)] were observed according to Campos [Campos, J.S.C. *et al.* (2007)]. These peaks correspond to α crystal phase.

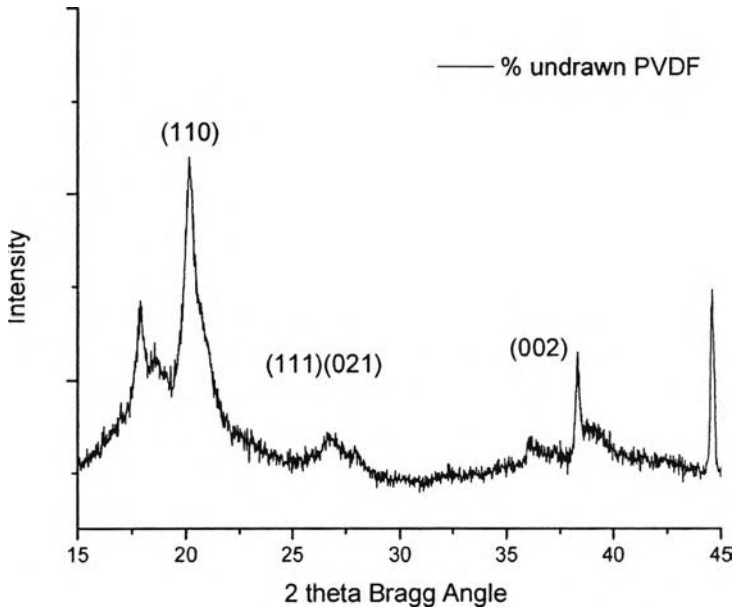

Figure 5.1 X-ray diffraction patterns of PVDF film.

The crystal phase and structure of $Ba_{0.7}Sr_{0.3}TiO_3$ were measured by XRD. Figure 5.2 shows the XRD spectrum of calcined $Ba_{0.7}Sr_{0.3}TiO_3$ at 800°C and 1000°C before sintering. XRD pattern shows sharp peaks around 32°, 40° and 45° [CHO, S.D. et al, (2004)] which belong to the barium titanate perovskite structure. It can be seen in calcining temperature at 800 °C that there are two little peak lines appearing at 24.18 ° and 34.4 ° corresponding to residual carbonates phase, such as $BaCO_3$, $SrCO_3$ and (Ba,Sr) CO_3. At higher calcining temperature, 1000 ° C, these peaks disappeared. These results indicate that when temperature increase, the $Ba_{0.7}Sr_{0.3}TiO_3$ formation via a solid state reaction between (Ba,Sr) CO_3 and amorphous TiO_2 is occurred. The XRD peak at 2θ ~ 46 ° show no splitting for calcining temperature of

$Ba_{0.7}Sr_{0.3}TiO_3$ at 800 °C and 1000 °C which can be indicated that $Ba_{0.7}Sr_{0.3}TiO_3$ is cubic structure [Ioachim, A. *et al.*, (2006)]. Lattice parameters of the calcined $Ba_{0.7}Sr_{0.3}TiO_3$ at 800 and 1000 °C before sintering rem ain almost constant (Table 5.1). After sintering at 1350 °C, XRD patterns of $Ba_{0.7}Sr_{0.3}TiO_3$ powder are the same as those of calcining (Figure 5.3). The $Ba_{0.7}Sr_{0.3}TiO_3$ powder after sintered at 1350 °C reveals tetragonal phase as observed by the splitting at $2\theta \sim 46$ °C. $Ba_{0.7}Sr_{0.3}TiO_3$ powder after sintered at 1350 °C shows changing of structure from cubic to tetragonal structure for both calcining temperature at 800 °C and 1000 °C. This can be explained from the fact that $Ba_{0.7}Sr_{0.3}TiO_3$ shows tetragonal after sintering process. $Ba_{0.7}Sr_{0.3}TiO_3$ after sintering shows that lattice parameter increase with increasing of calcining temperature (Table 5.2). This results may be explained by the atomic entities must have been in the non-equilibrium position which relaxes to the equilibrium position when annealed at higher temperature.

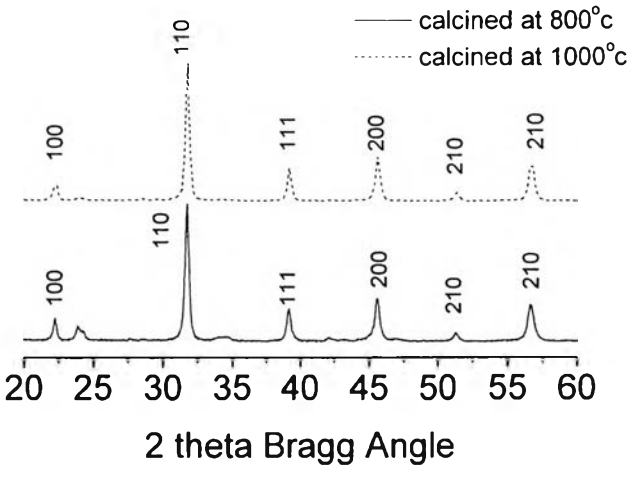

Figure 5.2 X-ray diffraction patterns of calcined $Ba_{0.7}Sr_{0.3}TiO_3$ at 800°C and 1000 °C.

Table 5.1 Lattice parameter of the calcined $Ba_{0.7}Sr_{0.3}TiO_3$ at 800°C and 1000 °C

Calcining Temperature °C	Unit cell parameter		Unit cell volume	Tetragonal
	a_0(nm)	c_0(nm)	v_0 x10^3(nm^3)	ratio c_0/a_0
800	0.39	0.39	59.31	1
1000	0.39	0.39	59.31	1

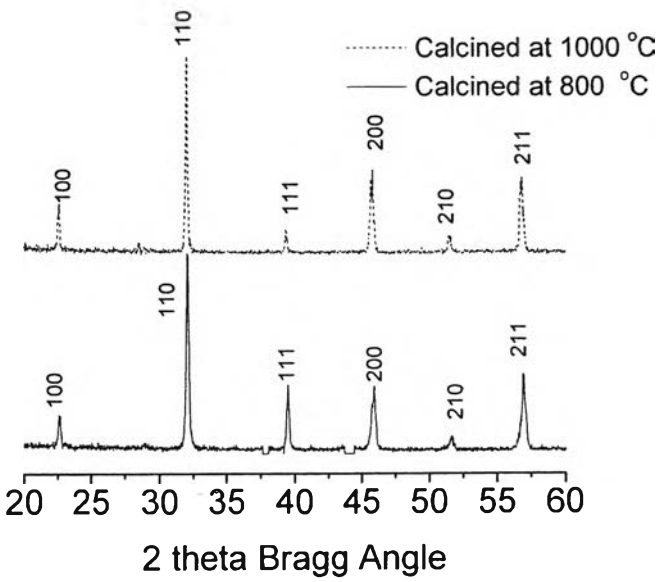

Figure 5.3 X-ray diffraction patterns of sintered $Ba_{0.7}Sr_{0.3}TiO_3$ at different calcined temperature 800°C and 1000 °C.

Table 5.2 Lattice parameter of the sintered $Ba_{0.7}Sr_{0.3}TiO_3$ at different calcined temperature 800°C and 1000°C after sintering

Calcining Temperature °C	Unit cell parameter		Unit cell volume	Tetragonal
	a_0(nm)	c_0(nm)	v_0 x10^3(nm^3)	ratio c_0/a_0
800	3.97	3.98	62.73	1.00
1000	3.99	3.95	62.88	0.98

Figure 5.4 presents the X-ray diffractograms of PVDF/$Ba_{0.7}Sr_{0.3}TiO_3$ composites in weight proportions of 100/0, 70/30, 50/50, 30/70 and 0/100. It was observed that when amount of $Ba_{0.7}Sr_{0.3}TiO_3$ increases in the composite, the intensity of the peak at 32 of 2θ obviously increases and the intensity of PVDF peaks tends to be disappeared. This disappearance is simply not implying to the absence of polymer but show the higher crystalline of $Ba_{0.7}Sr_{0.3}TiO_3$.

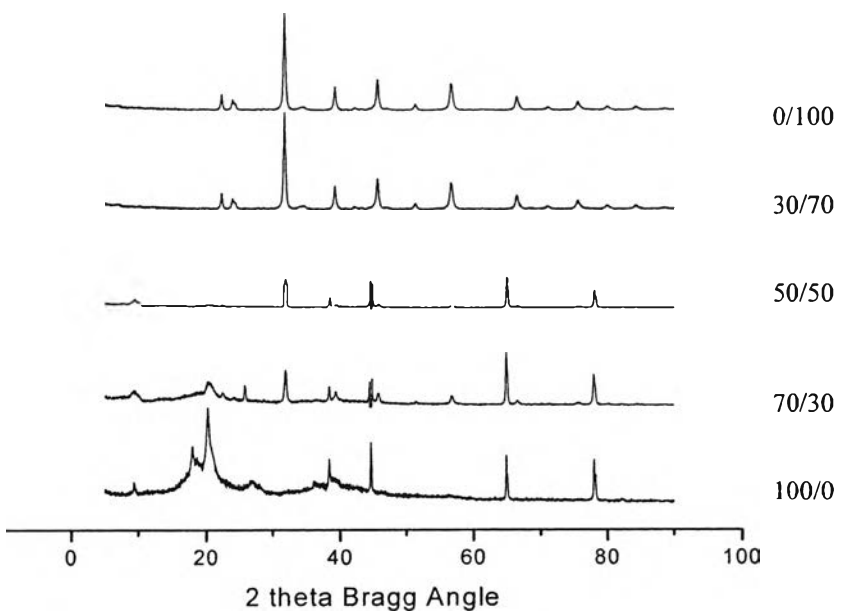

Figure 5.4 X-ray diffractrograms of PVDF/ $Ba_{0.7}Sr_{0.3}TiO_3$ composites in weight proportion of 100/0, 70/30, 50/50, 30/70 and 0/100.

5.4.2 Thermogravimetric analysis-TGA

Figure 5.5 shows the graphic of weight loss versus temperature for PVDF and $Ba_{0.7}Sr_{0.3}TiO_3$. The degradation of PVDF is observed at 400°C. The small weight loss of BST was observed at 100 °C which corresponds to the evaporate of water. For the weight loss at 600 °C corresponds to result from inflammation of residual organic compounds.

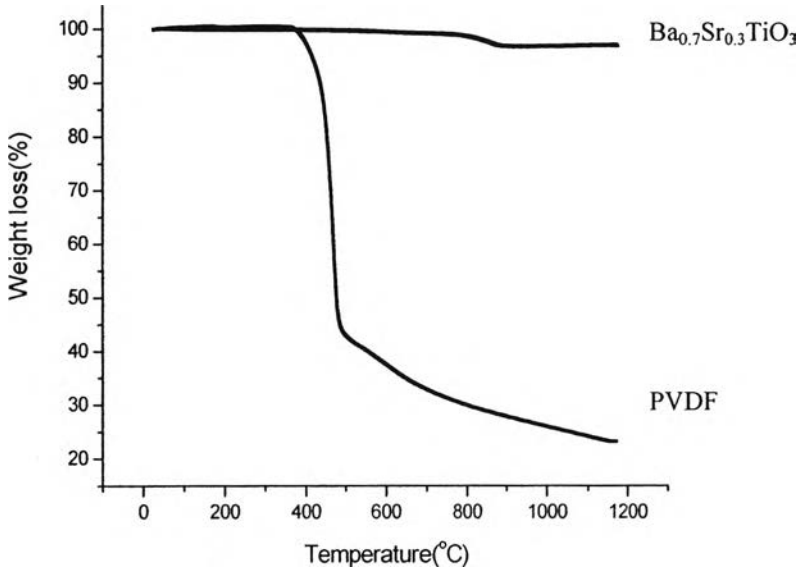

Figure 5.5 Weight loss (%) in function of the temperature (° C) for PVDF Polymer and $Ba_{0.7}Sr_{0.3}TiO_3$ powder.

Figure 5.6 shows the TGA thermograms of PVDF/$Ba_{0.7}Sr_{0.3}TiO_3$ composites, in weight proportions of 100/0, 70/30, 50/50, 30/70 and 0/100. In Figure 5.6 and Table 5.3 show that the incorporation of $Ba_{0.7}Sr_{0.3}TiO_3$ in the PVDF films enhances the higher thermal stability of composite when compared to the pure PVDF.

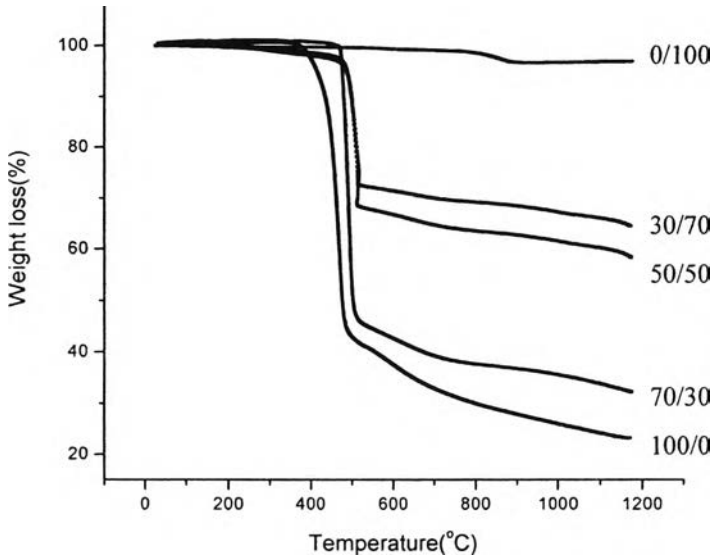

Figure 5.6 TGA thermo grams of PVDF/ $Ba_{0.7}Sr_{0.3}TiO_3$ composites in weight proportions of 100/0, 70/30, 50/50, 30/70 and 0/100.

Table 5.3 Decomposition of PVDF/$Ba_{0.7}Sr_{0.3}TiO_3$ at different % weight

Materials	Decomposition Temperature °C
Pure PVDF	468
PVDF 70% by weight	493
PVDF 50% by weight	508
PVDF 30% by weight	512

5.4.3 Differential scanning calorimetry-DSC

Figure 5.7 shows the graph of heat flow versus temperature for PVDF/ $Ba_{0.7}Sr_{0.3}TiO_3$ composites, in weight proportions of 100/0, 70/30, 50/50 and 30/70. It is observed that PVDF and composites show endothermic melting peaks around 170 °C. This behavior verifies that $Ba_{0.7}Sr_{0.3}TiO_3$ does not influence in the melting temperature of PVDF due to weak interactions between PVDF and $Ba_{0.7}Sr_{0.3}TiO_3$ composites. It is noticed that PVDF and PVDF/ $Ba_{0.7}Sr_{0.3}TiO_3$ composites do not undergo weight loss after the melting temperature confirming the good thermal stability of them by TGA.

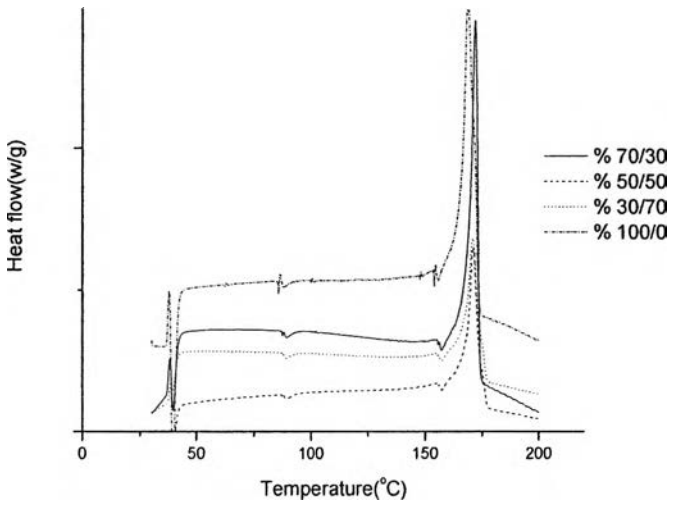

Figure 5.7 DSC thermograms of PVDF/ $Ba_{0.7}Sr_{0.3}TiO_3$ in weight proportions 100/0, 70/30, 50/50 and 30/70.

5.4.4 Scanning electron microscopes-SEM

SEM image shows that the particle size of $Ba_{0.7}Sr_{0.3}TiO_3$ before sintering is larger with higher calcining temperature (Figure 5.8). After sintering, the particle coalesce to form large well defined crystallite and the grain size of $Ba_{0.7}Sr_{0.3}TiO_3$ increases with calcining temperature (Figure 5.9).

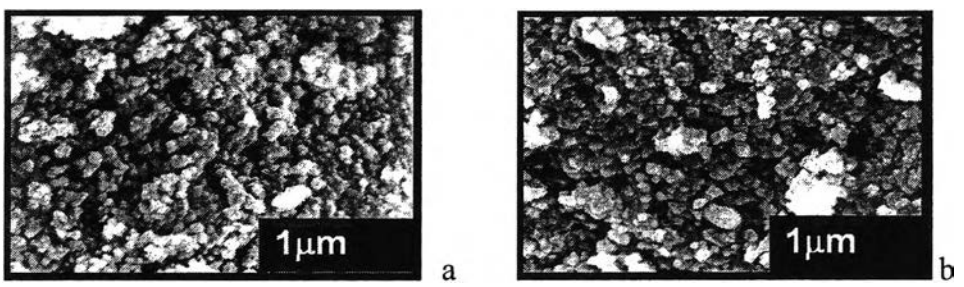

Figure 5.8 Scanning electron microscope (SEM) of the calcined $Ba_{0.7}Sr_{0.3}TiO_3$ at (a) 800 °C and (b) 1000 °C before sintering.

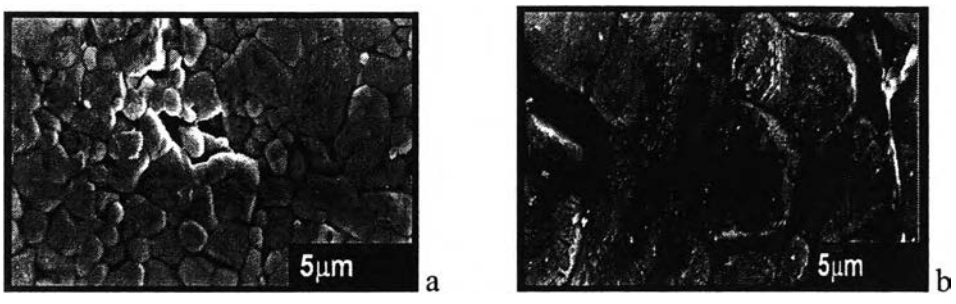

Figure 5.9 Scanning electron microscope (SEM) of the sintered $Ba_{0.7}Sr_{0.3}TiO_3$ calcining at (a) 800°C and (b) 1000°C.

The SEM surface micrographs of PVDF/$Ba_{0.7}Sr_{0.3}TiO_3$ at weight proportions 100/0, 70/30, 50/50 and 30/70 was clearly seen that the $Ba_{0.7}Sr_{0.3}TiO_3$ particles had a connectivity zero while the PVDF polymer had a connectivity of 3 which shown in Figure 5.10. However, the images show homogeneous images at 70/30 and tend to show larger agglomeration when increasing weight fraction of $Ba_{0.7}Sr_{0.3}TiO_3$ particles which may occur due to Van der Waals force of BST molecule attract the another molecule.

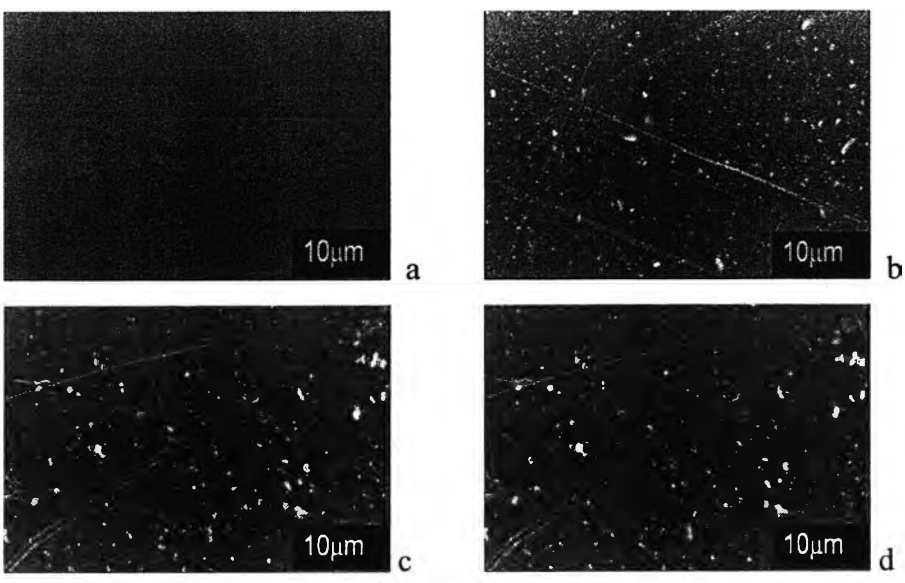

Figure 5.10 Scanning electron microscope (SEM) of the PVDF/ $Ba_{0.7}Sr_{0.3}TiO_3$ composites at weight proportions of (a) 100/0 (b) 70/30, (c) 50/50 and (d) 30/70.

5.4.5 Transmission electron microscopes -TEM

The particle size of $Ba_{0.7}Sr_{0.3}TiO_3$ is investigated by TEM. Figure 5.11 show TEM images of particles obtained from calcining at 800 °C and 1000 °C. The large particle size is observed with increasing of calcining temperature. At calcining temperature at 800 °C and 1000 °C, the average particle diameters are found to be approximately 30-40 nm and 50-60 nm respectively.

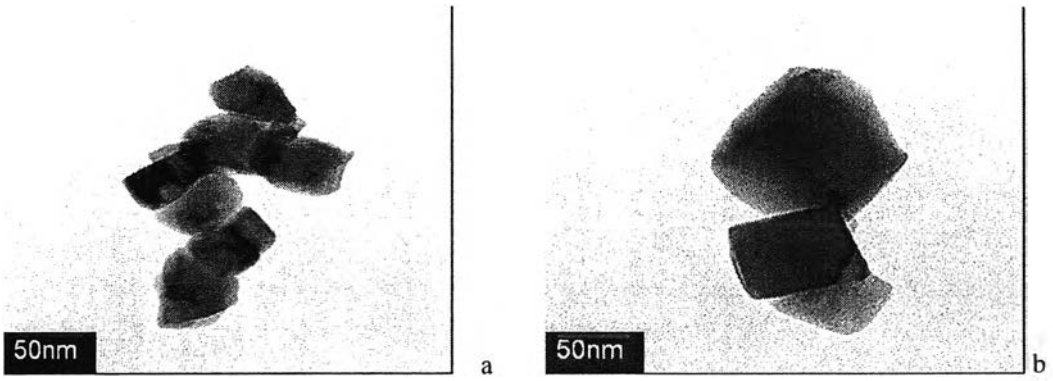

Figure 5.11 Transmission electron microscopes (TEM) of calcined $Ba_{0.7}Sr_{0.3}TiO_3$ at (a) 800°C and (b)1000°C.

5.4.6 Dielectric measurement

Figure 5.12 and Figure 5.13 show the variation of dielectric constant and the loss tangent with applied electric field of the sintered $Ba_{0.7}Sr_{0.3}TiO_3$ at different calcining temperatures. The higher dielectric constant is found in the sample with higher calcining temperature as results from the larger grain size. The dielectric loss increase with increasing grain size [Nayak, M. et al.,(2002)] which can be seen that $Ba_{0.7}Sr_{0.3}TiO_3$ at calcining temperature of 1000 °C shows higher loss tangent than $Ba_{0.7}Sr_{0.3}TiO_3$ at calcining temperature of 800 °C

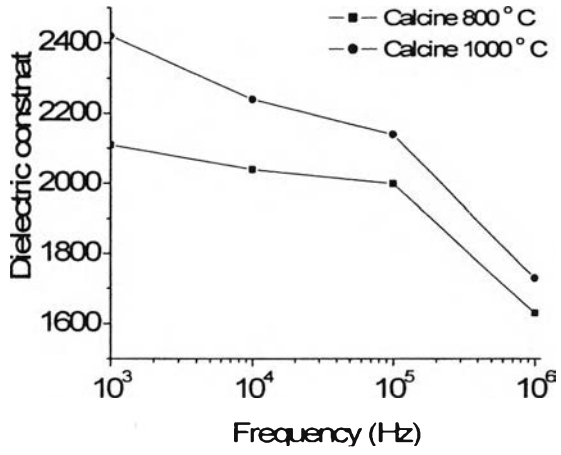

Figure 5.12 The frequency dependence of the dielectric constant of sintered $Ba_{0.7}Sr_{0.3}TiO_3$ at 1350 °C at different calcining temperatures.

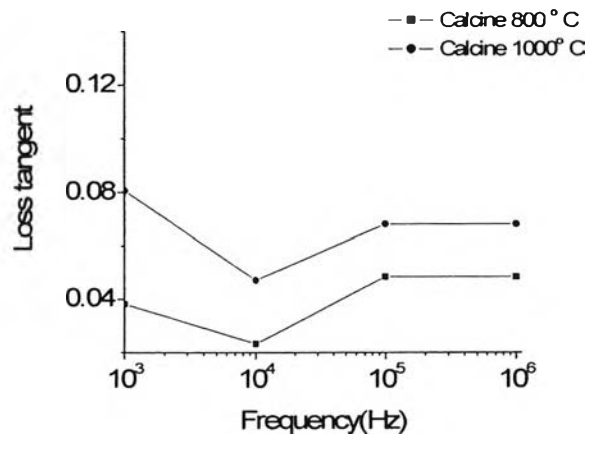

Figure 5.13 The frequency dependence of the dielectric loss tangent of sintered $Ba_{0.7}Sr_{0.3}TiO_3$ at 1350 °C at different calcining temperatures.

The effects of temperature on the dielectric constant of the ceramics are also investigated. Figure 5.14 show the variation of dielectric constant of the $Ba_{0.7}Sr_{0.3}TiO_3$ ceramics (calcined 800°C) with temperature at different frequency. From this graph, the $Ba_{0.7}Sr_{0.3}TiO_3$ ceramic shows a peak at 40 °C indicated curie temperature as a phase transition from ferroelectric to paraelectric phase. Therefore, the $Ba_{0.7}Sr_{0.3}TiO_3$ ceramic can use in ferroelectric application at temperature up to 40 °C.

Figure 5.15 shows the variation of dielectric loss tangent of the $Ba_{0.7}Sr_{0.3}TiO_3$ ceramics (calcined 800°C) with temperature at different frequency which was lower than 0.3 at all temperatures and all frequencies.

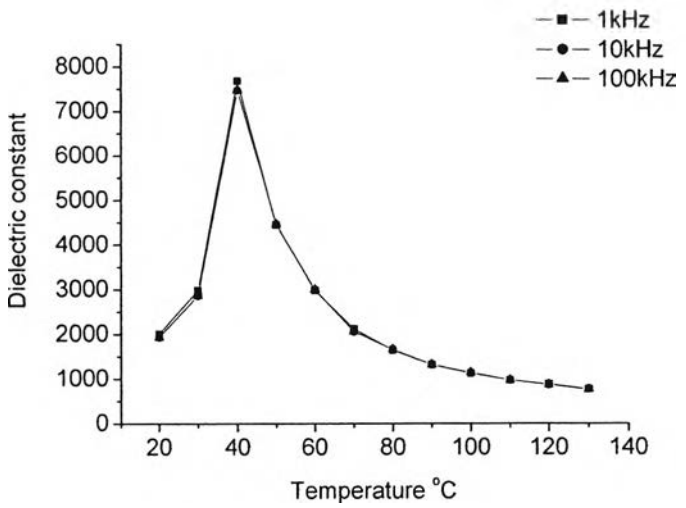

Figure 5.14 The temperature dependence of the dielectric constant of sintered $Ba_{0.7}Sr_{0.3}TiO_3$ at 1350 °C at different frequencies.

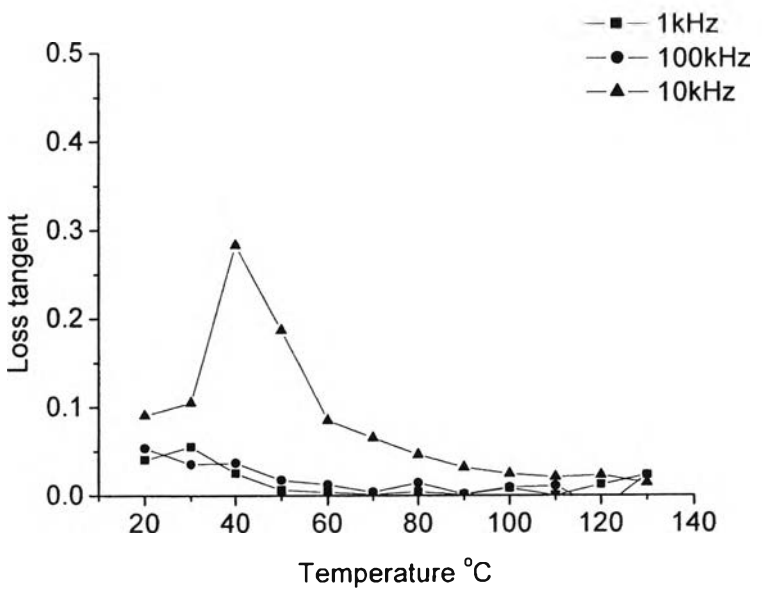

Figure 5.15 The temperature dependence of the dielectric loss tangent of sintered $Ba_{0.7}Sr_{0.3}TiO_3$ at 1350 °C at different frequency.

The frequency dependant dielectric constant of PVDF/calcined $Ba_{0.7}Sr_{0.3}TiO_3$ at 800°C composites is shown in Figure 5.16 The dielectric constant was very large, about 21.4 at 10^3 Hz and at weight fraction of 30/70. However, it is obviously noticed that the value of dielectric constant increases with increasing in weight fraction from 100/0 to 30/70 because of the high dielectric constant of $Ba_{0.7}Sr_{0.3}TiO_3$. Figure 5.17 shows the dielectric lose tangent which lower than 0.1 at frequency up to1 MHz for all composition.

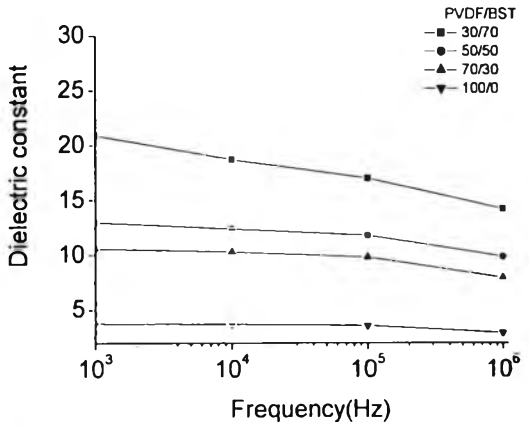

Figure 5.16 The frequency dependence of the dielectric constant of PVDF/calcined $Ba_{0.7}Sr_{0.3}TiO_3$ at 800°C composites in weight proportions of 100/0, 70/30, 50/50 and 30/70.

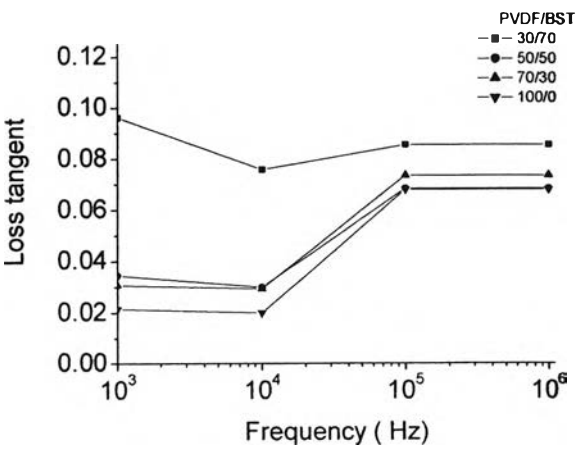

Figure 5.17 The frequency dependence of the dielectric loss tangent of PVDF/calcined $Ba_{0.7}Sr_{0.3}TiO_3$ at 800°C composites in weight proportions of 100/0, 70/30, 50/50 and 30/70.

Figure 5.18 shows dielectric constant of PVDF/$Ba_{0.7}Sr_{0.3}TiO_3$ (30/70) composites at different calcined temperatures for $Ba_{0.7}Sr_{0.3}TiO_3$. High dielectric constant, about 24.4 at 10 kHz, was observed for PVDF/ $Ba_{0.7}Sr_{0.3}TiO_3$ calcined at 1000 °C. However, it is obviously noticed that the dielectric constant value increases with increasing of calcining temperature from 800 °C to 1000 °C. The increase in dielectric constant with increasing calcining temperature is attributed to the increase in the grain size of $Ba_{0.7}Sr_{0.3}TiO_3$. From Figure 5.19, the dielectric loss tangent shows lower than 0.1 at frequency up to 1 MHz for both samples.

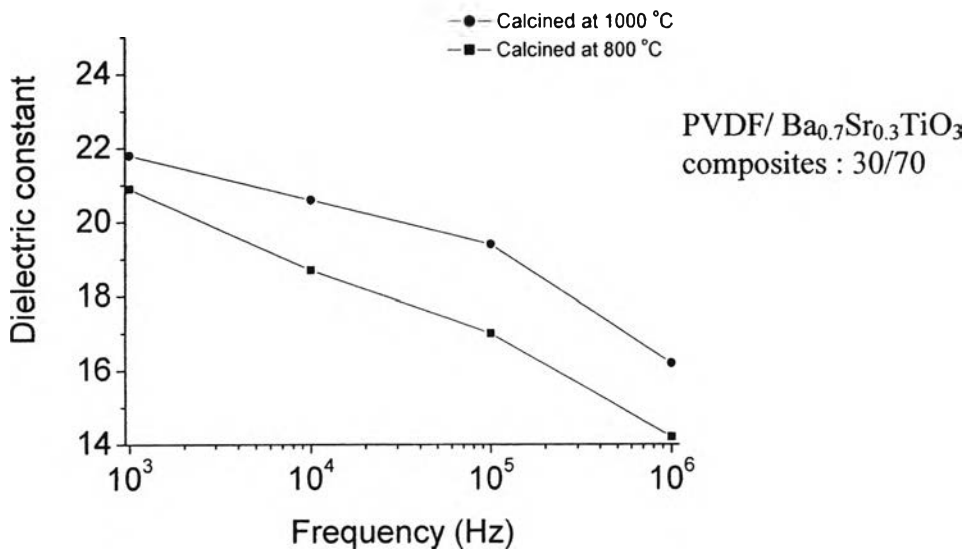

Figure 5.18 The frequency dependence of the dielectric constant of PVDF/ $Ba_{0.7}Sr_{0.3}TiO_3$ composites at different calcining temperature.

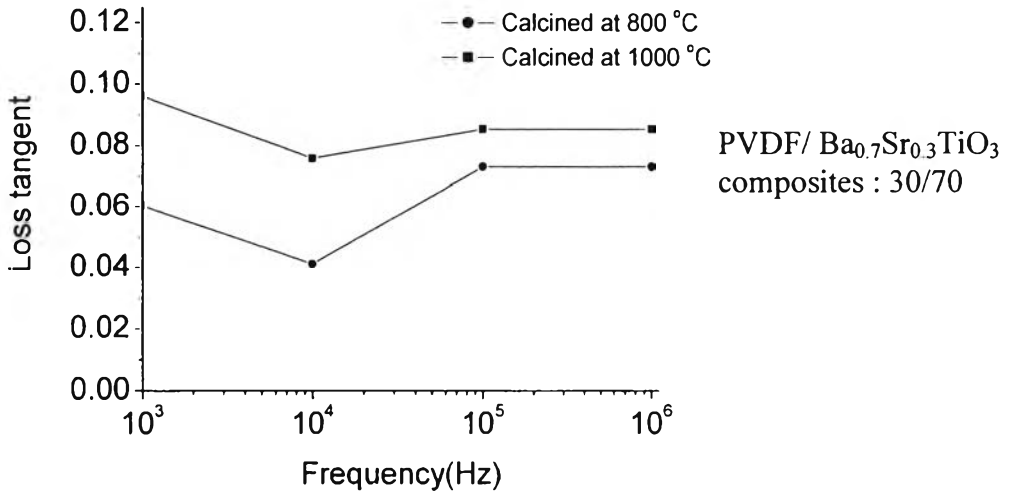

Figure 5.19 The frequency dependence of the dielectric loss tangent of PVDF/ $Ba_{0.7}Sr_{0.3}TiO_3$ composites at different calcining temperature.

The temperature dependent of dielectric constant of the PVDF/ $Ba_{0.7}Sr_{0.3}TiO_3$ (calcined 800°C) composites were also investigated. Figure 5.20 shows the variation of dielectric constant of the PVDF/ $Ba_{0.7}Sr_{0.3}TiO_3$ composites with temperature at 1 kHz. From this graph, it should be observed that the dielectric of the composites is not stable with temperature and might reach a peak at acertain temperature higher than the measurement range.

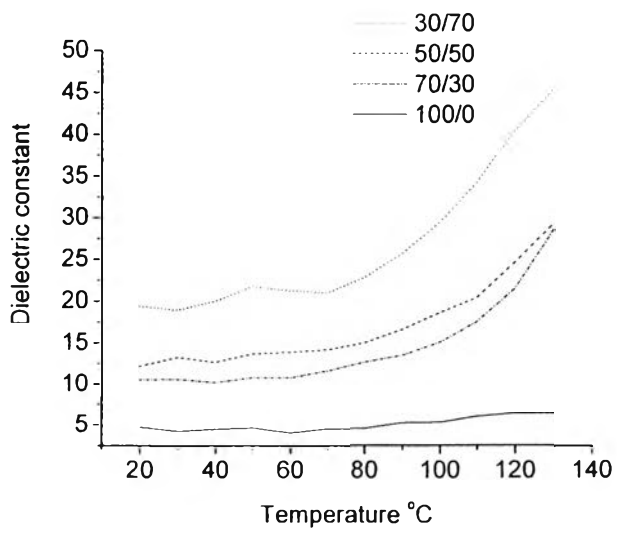

Figure 5.20 The temperature dependence of the dielectric constant of PVDF/ $Ba_{0.7}Sr_{0.3}TiO_3$ composites at 1 kHz.

4.5 Conclusion

The PVDF/ $Ba_{0.7}Sr_{0.3}TiO_3$ composite with 0-3 connectivity were successfully fabricated. The high content of $Ba_{0.7}Sr_{0.3}TiO_3$ in the composite shows increased crystalline phase of ceramics and the intensity of PVDF peaks tends to be disappeared. The $Ba_{0.7}Sr_{0.3}TiO_3$ powders were derived from sol-gel process at different calcining temperatures dispersed in PVDF matrix; however, more agglomeration were found in composites at high $Ba_{0.7}Sr_{0.3}TiO_3$ content (70%wt). It was found that increasing the amount of ceramic powders in composites and the temperature of calcine ceramic powders enhance the dielectric constant of composites. The application of composite depends on temperature because the dielectric constant of composite does not remain constant with temperature. Also the thermal stability of the composites can be improved by higher amount of ceramic powders but melting temperature of composite does not change compared to pristine PVDF.

Acknowledgements

The authors wish to thank MTEC staffs as electronic measurement for useful assistance and instrument for characterizations. The partial funding of research work was provided by PPT consortium and Polymer Processing and Nanomaterials research unit.

Referrence

Campos, J.S.C., Ribeiro, A.A., Cardoso, C.X. (2007) Preparation of characterization of PVDF/$CaCO_3$ composites. Journal of Materials Science& Engineering B, 136, pp 123-128

Lu, Q., Chen, D., and Jiao, X. (2003) Preparation and characterization of Ba Sr TiO (x=0.1, 0.2) fibers by sol–gel process using catechol-complexed titanium isopropoxide, Journal of Alloys and Compounds, 358, 76–81.

Mao, C., Dong, X., Zeng,T. Chen, H. Cao, F. (2006) Nonhydrolytic sol-gel synthesis and dielectric properties of ultrafine-grained and homogenized $Ba_{0.7}Sr_{0.3}TiO_3$, Ceramic International, xxx, pp xxx

Mohammadi, B., Yousefi, A.A., Bellah, S. M. (2007) Effect of tensile strain rate and elongation on crystalline structure and piezoelectric properties of PVDF thin films, Polymer Testing, 26, pp 42-50.

Nayak, M., Lee, S.Y., and Tseng, T.Y. (2002) Electrical and dielectric properties of $(Ba_{0.5}Sr_{0.5})TiO_3$ thin films prepared by a hydroxide–alkoxide precursor-based sol–gel method, Materials Chemistry and Physics, 77, 34–42.

Olszowy, M. (1997) Piezoelectricity and Dielectric Properties of PVDF/$BaTiO_3$ Composites, Journal of Der Spiegel, 3181, 69-72.

Wua, D., Li, A., Ling, H., Yin, X., Ge, C., Wang, M., Ming, N. (2000) Preparation $(Ba_{0.5}Sr_{0.5})TiO_3$ thin films by sol–gel method with rapid thermal annealing. Journal of Applied Surface Science, 165, 309–314.

Ye, Y., Jiang, Z., Wu, Y., Zwng, H., Yang, Y. and Li W (2004) Characterization and Ferroelectric Properties of Electric Poled PVDF Films, School of optoelectronic Information, University of Electric Science and Technology of China.